RSC Advances

PAPER

View Article Online
View Journal | View Issue

Cite this: *RSC Adv.*, 2022, **12**, 22295

Altereporenes A–E, five epoxy octa-hydronaphthalene polyketides produced by an endophytic fungus *Alternaria* sp. YUD20002†

Dan-Dan Xia,[a] Hao-Jie Duan,[a] Fei Xie,[a] Tian-Peng Xie,[a] Yan Zhang,[a] Yue Sun,[a] Jian-Mei Lu,[a] Yu-Hong Gao,[c] Hao Zhou *[a] and Zhong-Tao Ding *[ab]

Received 25th June 2022
Accepted 22nd July 2022

DOI: 10.1039/d2ra03917f

rsc.li/rsc-advances

Five previously undescribed epoxy octa-hydronaphthalene polyketides, altereporenes A–E (**1–5**) were isolated from rice culture of the endophytic fungus *Alternaria* sp. YUD20002 derived from the tubers of *Solanum tuberosum*. Their structures were determined on the basis of comprehensive spectroscopic analyses, while the absolute configurations were elucidated by the comparison of experimental and calculated specific rotations. Meanwhile, the antimicrobial, cytotoxic, anti-inflammatory and acetylcholinesterase inhibitory activities of compounds **1–5** were also investigated.

Introduction

Endophytic fungi, unique microorganisms that can asymptomatically colonize the living tissues of healthy plants,[1,2] have been recognized as vital sources of novel natural products and attracted extensive attention owing to their intriguing new structures with prominent biological activities.[3–8] In particular, *Alternaria*-related fungi have been reported to produce bioactive and structurally diverse secondary metabolites in recent years.[9–11] As far as we know, previous studies on the genus *Alternaria* have resulted in the isolation of numerous metabolites with various novel skeletons including the hydroanthraquinone derivatives,[12] benzopyrone derivatives,[13] diterpenoids,[14,15] α-pyrone derivatives,[16] *etc.*

In order to explore structural diversity natural products from the endophytic fungi, the chemical investigation of the secondary metabolites from *Alternaria* sp. YUD20002 which was derived from *Solanum tuberosum* (potato) was carried out. Further scale-up fermentation followed by chemical investigation of the secondary metabolites of the strain yielded five new compounds, altereporenes A–E (**1–5**). Their structures (Fig. 1) were characterized as complex epoxy octa-hydronaphthalene analogues coupled with different side chains by spectroscopic data analysis and quantum chemical calculated. In this work, the isolation, structural elucidation, and bioactivity of these compounds were described.

Results and discussion

Altereporene A (**1**) was isolated as a white amorphous powder and the molecular formula $C_{23}H_{34}O_4$ was determined by its HRESIMS (*m/z* 397.2350 $[M + Na]^+$, calcd for 397.2349), indicating seven degrees of unsaturation. The ^{13}C NMR data (Table 1) indicated 23 carbon signals, and based on the DEPT spectra, these carbons were classified as four methyls, four methylenes (including an oxygenated one at δ_C 62.6), five olefinic methines, six sp^3 methines (including three oxygenated ones at δ_C 60.0, 62.2, and 66.0), one oxygen-bearing quaternary carbon (δ_C 78.5), and three olefinic quaternary carbons. The ^1H and ^{13}C NMR spectra of **1** (Tables 1 and 2) revealed it was tricyclic and possessed four double bond to satisfy its unsaturation requirements. These data indicated that the structural features of constituent **1** arising from its 1D NMR spectra were similar to those of anthracobic acid A, a polyketide from *Anthracobia* sp.[17] The detailed planar structure of **1** was further constructed based on the ^1H–^1H COSY and HMBC spectra (Fig. 2). The ^1H–^1H COSY spectrum indicated the presence of four independent spin systems, H_2-1/H_2-2/H_2-3(A), H-5/H-6/H-7/H-8/H-9(H-10/H-11)/H-14/H_2-13(B), H-15/H-16(C) and H-19/H_3-20(D). Spin systems A and B were confirmed to be connected through the quaternary olefinic carbons (C-4) *via* the HMBC correlations of H_3-21 to C-3/C-4/C-5 and H-3 to C-4/C-5. Meanwhile, the chemical shift of C-1 (δ_C 62.6) illustrated a hydroxyl group linked to C-1. The HMBC correlations, especially those from H_3-22 to C-11/C-12/C-13, from H_a-13 to C-9/C-11/C-12/C-14, combined with the chemical shift of C-10 (δ_C 66.0) deduced the presence of a methylcyclohexene skeleton with a hydroxyl at C-10. The HMBC correlations from H-15 to C-9/C-13/C-14, from

[a]*Key Laboratory of Functional Molecules Analysis and Biotransformation of Universities in Yunnan Province, School of Chemical Science and Technology, Yunnan University, Kunming, 650091, China. E-mail: Haozhou@ynu.edu.cn; ztding@ynu.edu.cn*

[b]*College of Pharmacy, Dali University, Dali, 671000, China*

[c]*The First People's Hospital of Yunnan Province, Kunming, 650034, China*

† Electronic supplementary information (ESI) available. See https://doi.org/10.1039/d2ra03917f

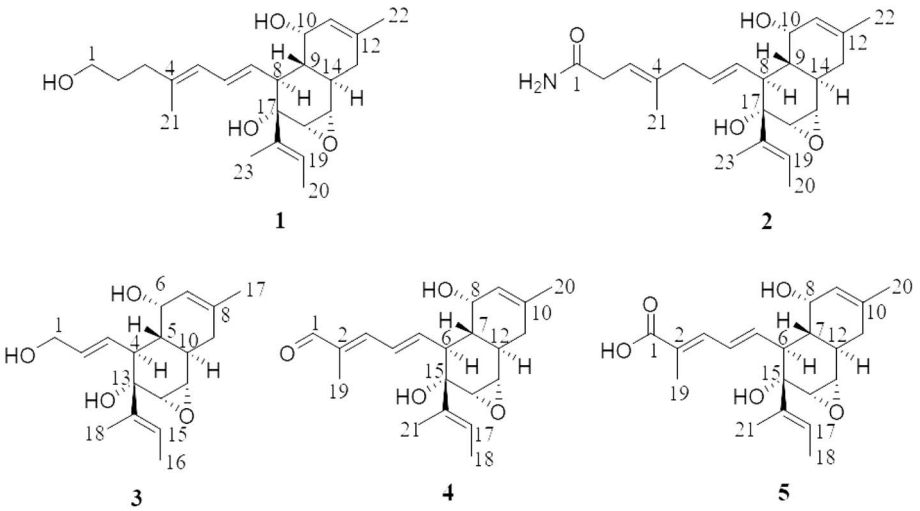

Fig. 1 Chemical structures of compounds **1**–**5**.

Table 1 ^{13}C NMR spectroscopic data of compounds **1**–**5** (δ in ppm)[a]

Pos.	1	2	3	4	5
1	62.6, CH_2	177.8, C	63.8, CH_2	197.3, C	179.5, C
2	32.0, CH_2	36.0, CH_2	133.9, CH	137.5, C	130.3, C
3	37.1, CH_2	118.7, CH	130.6, CH	151.2, CH	138.4, CH
4	137.4, C	139.8, C	47.2, CH	130.4, CH	130.9, CH
5	126.5, CH	43.9, CH_2	43.2, CH	145.3, CH	139.1, CH
6	131.3, CH	132.6, CH	65.7, CH	48.3, CH	48.0, CH
7	130.5, CH	130.5, CH	125.5, CH	43.6, CH	43.5, CH
8	47.5, CH	47.3, CH	139.3, C	66.0, CH	65.9, CH
9	43.8, CH	43.3, CH	37.0, CH	125.5, CH	125.6, CH
10	66.0, CH	66.0, CH	30.4, CH	139.3, C	139.8, C
11	125.6, CH	125.6, CH	59.9, CH	36.9, CH_2	37.0, CH_2
12	139.2, C	139.2, C	62.1, CH	30.4, CH	30.3, CH
13	37.1, CH_2	37.0, CH_2	78.3, C	59.9, CH	60.0, CH
14	30.3, CH	30.3, CH	138.5, C	62.2, CH	62.2, CH
15	60.0, CH	60.0, CH	123.8, CH	78.6, C	78.5, C
16	62.2, CH	62.2, CH	13.7, CH_3	138.1, C	139.0, C
17	78.5, C	78.3, C	23.4, CH_3	124.4, CH	124.0, CH
18	138.7, C	138.6, C	14.8, CH_3	13.7, CH_3	13.7, CH_3
19	123.6, CH	123.7, CH		9.4, CH_3	13.5, CH_3
20	13.7, CH_3	13.7,CH_3		23.4, CH_3	23.4, CH_3
21	16.7, CH_3	16.8, CH_3		14.8, CH_3	14.8, CH_3
22	23.4, CH_3	23.4, CH_3			
23	14.8, CH_3	14.9, CH_3			

[a] Measured at 400 MHz in methanol-d_4.

H-16 to C-8/C-15/C-17, and from H-8 to C-17 suggested the spin systems B and C were comprised of an octa-hydronaphthalene skeleton. Based on the analyses above together with the HMBC correlations from H_3-23 to C-17/C-18/C-19, from H_3-20 to C-18/C-19, and from H-19 to C-17, along with the chemical shift of C-17 (δ_C 78.5), indicating that the 2-butene moiety was connected to the oxygenated quaternary carbon (C-17). Furthermore, the presence of an epoxy group at C-15 and C-16 were assigned by the molecular formula and the chemical shifts of the ^{13}C-NMR data of these positions. Thus, the planar structure of **1** was provided.

The relative configuration of **1** was established by the coupling constants and NOESY correlations (Fig. 3). The *trans*-orientations of C_4–C_5 and C_6–C_7 were determined by the coupling constant of $J_{H\text{-}6/H\text{-}7}$ at 15.0 Hz, and NOESY correlations of H-5/H-7, H-6/H_3-21. In addition, the NOESY correlation between H-19 and H-16, along with the lack of obvious correlation between H-23 and H-16, indicated that the configuration of the double bond C_{18}–C_{19} should also be *trans*-orientation. The NOESY correlations of H-7/H-9/H-10, H-9/H-15/H-16, and H-16/H-19 suggested that the protons H-9, H-10, H-15, H-16 and H-19 were on the same side and were randomly assigned α-orientation, while the NOESY correlation between H-8 and H-14 assigned H-8 and H-14 on β-orientation of the molecule. The above analysis supported the presence of two possible isomers, (8*S*, 9*R*, 10*S*, 14*R*, 15*S*, 16*S*, 17*S*)-**1** and (8*R*, 9*S*, 10*R*, 14*S*, 15*R*, 16*R*, 17*R*)-**1**. To determine its absolute configuration, TDDFT-ECD calculations were performed at the B3LYP/6-31g (d, p) level in methanol.[18–21] However, neither of the calculated ECD curves for two possible isomers of **1** matched well with the experimental curves. Finally, the absolute configuration of **1** was elucidated by comparison of the experimental and the theoretical value of specific rotations. Each isomer was optimized at the B3LYP/6-31g (d, p) level in methanol using DFT in the Gaussian 09 program. Then, the optimized isomer was calculated using TDDFT/GIAOs at the B3LYP/6-31g* in the Gaussian 09 program to generate its specific rotation. As expected, the calculated specific rotation ([*a*] −223.67) was perfectly matched to the experimental one ([*a*] −121.0). Therefore, the absolute configuration of **1** was established as 8*S*, 9*R*, 10*S*, 14*R*, 15*S*, 16*S*, 17*S*, and named as altereporene A.

Altereporene B (**2**), obtained as a yellowish-green solid, possessed a molecular formula of $C_{23}H_{33}NO_4$ with eight index of hydrogen deficiency based on the positive mode with an obvious HRESIMS ion peak found at *m/z* 410.2301 $[M + Na]^+$ (calcd for 410.2302). The ^{13}C NMR (Table 1) spectrum of **2** displayed resonances for 23 carbons ascribed to four methyls, three methylenes, eleven methines, and five quaternary carbons

Table 2 ^{1}H NMR spectroscopic data of compounds **1–5** (δ in ppm, J in Hz)[a]

Pos.	1	2	3	4	5
1	3.53, t (6.6)		4.04, m	9.39, s	
2	1.63, overlap	2.95, d (7.4)	5.74, dt (15.3, 6.3)		
3	2.10, t (7.1)	5.39, m	5.22, dd (15.3, 10.4)	6.99, d (11.3)	7.08, d (11.4)
4			2.39, t (11.6)	6.77, dd (14.9, 11.3)	6.55, dd (14.8, 11.3)
5	5.83, d (10.9)	2.75, d (6.7)	1.38, td (11.8, 3.0)	5.91, dd (15.0, 10.6)	5.56, overlap
6	6.42, dd (15.0, 10.9)	5.60, dt (15.2, 6.8)	3.84, dd (4.2, 3.4)	2.62, t (11.8)	2.53, t (11.2)
7	5.06, dd (15.0, 10.3)	4.97, dd (15.2, 10.4)	5.53, m	1.51, td (11.8, 3.0)	1.45, td (11.8,3.0)
8	2.40, t (11.8)	2.36, t (11.8)		3.78, dd (6.0, 2.9)	3.79, dd (5.0, 3.7)
9	1.37, td (11.8, 3.1)	1.34, td (11.8, 3.0)	2.20, m	5.54, overlap	5.53, overlap
			1.90, m		
10	3.81, dd (5.8, 3.5)	3.83, dd (4.4, 3.0)	2.14, m		
11	5.53, d (5.6)	5.54, m	3.17, d (3.8)	2.25, m	2.23, m
				1.94, m	1.93, m
12			3.08, d (3.7)	2.20, m	2.18, m
13	2.20, m	2.21, m		3.21, d (3.8)	3.19, d (3.8)
	1.90, m	1.90, m			
14	2.17, m	2.16, m		3.11, d (3.8)	3.10, d (3.8)
15	3.17, d (3.8)	3.16, d (3.8)	5.48, m		
16	3.08, d (3.8)	3.07, d (3.8)	1.67, overlap		
17			1.74, s	5.54, overlap	5.5, overlap
18			1.68, overlap	1.71, overlap	1.70, overlap
19	5.47, m	5.47, m		1.83, s	1.93, overlap
20	1.68, m	1.66, overlap		1.75, s	1.74, s
21	1.77, s	1.68, overlap		1.69, overlap	1.68, overlap
22	1.73, s	1.73, s			
23	1.67, m	1.69, overlap			

[a] Measured at 400 MHz in methanol-d_4.

including three olefinic ones, an amide carbonyl, as well as an oxygenated carbon. A comparison of its 1D (Tables 1 and 2) and 2D NMR (Fig. 2) data with compound **1** indicated that **2** should share a very similar structural core with **1**. One of the main differences between them was that the hydroxymethyl of C-1 in **1** was replaced by an amide group in **2**, which could be

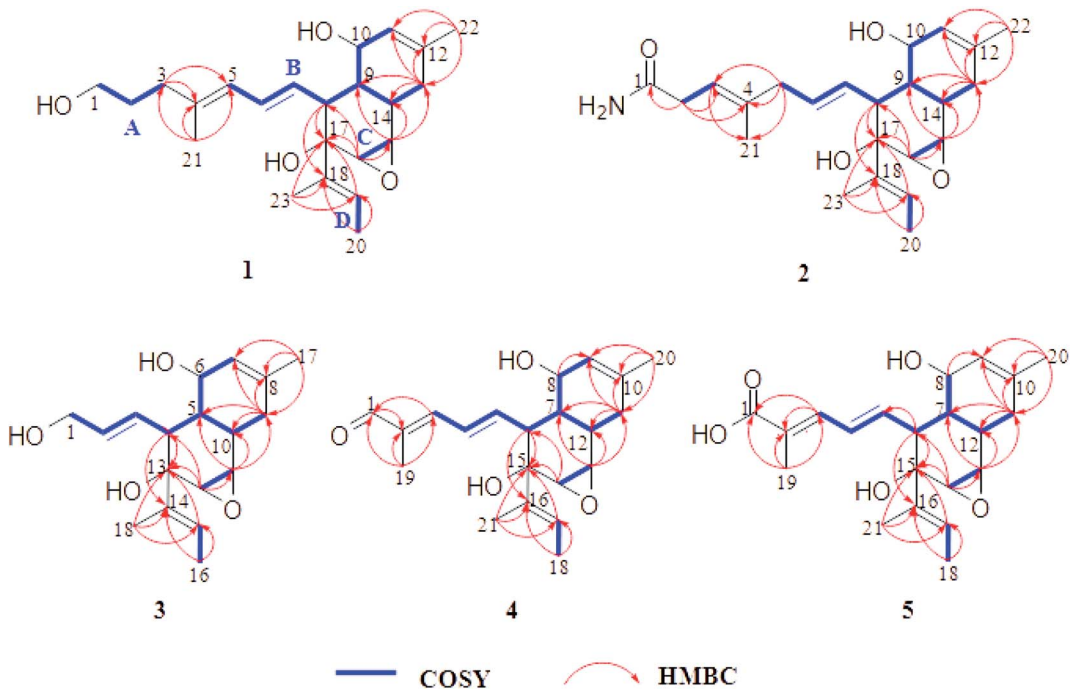

Fig. 2 The key ^{1}H–^{1}H COSY and HMBC correlations of compounds **1–5**.

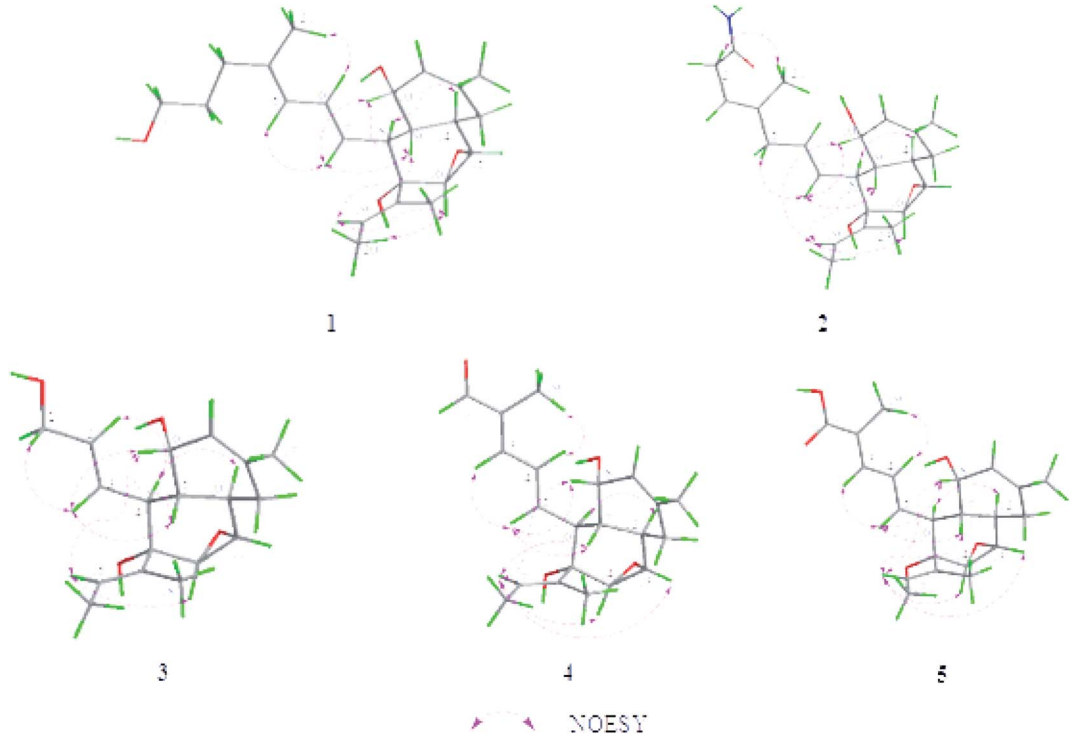

Fig. 3 Key NOESY correlations and the lowest energy state models of compounds **1–5** at B3LYP/6-31g (d, p) in methanol.

confirmed by the key HMBC correlations (Fig. 2) from H_2-2 to C-1. The HMBC correlations from H_2-2 to C-3/C-4, from H-3 to C-21, and from H_2-5 to C-3/C-4/C-21 suggested the double bond of C-4/C-5 in **1** migrated to C-3/C-4 in **2**. Collectively, the planar structure of **2** was illustrated.

The configurations of the *trans*-orientations of C_3–C_4, C_6–C_7 and C_{18}–C_{19} in **2** were also determined by the coupling constants of $J_{H\text{-}6/H\text{-}7}$ at 15.2 Hz, the NOESY correlations of H_2-2/H_3-21, H-5/H-7, H-19/H-16, together with the lack of obvious NOE correlation between H-23 and H-16 (Fig. 3). In the NOESY spectrum, the key cross-peaks between H-7 and H-9/H-10, H-19 and H-9/H-10/H-16, with the addition of H-8 and H-14 indicated that H-9, H-10, H-15, H-16 and the 2-butene moiety were on the same orientation, while H-8, H-14, and the epoxy group were on the opposite orientation. The above data limited the possible enantiomers to (8*S*, 9*R*, 10*S*, 14*R*, 15*S*, 16*S*, 17*S*)-**2** and (8*R*, 9*S*, 10*R*, 14*S*, 15*R*, 16*R*, 17*R*)-**2**. Then, the absolute configuration of **2** was also determined to be the same 8*S*, 9*R*, 10*S*, 14*R*, 15*S*, 16*S*, 17*S* as that of **1** by specific rotation calculation, both experimental and theoretical specific rotations of **2** were negative. Accordingly, the structure of **2** was defined as shown (Fig. 1), and named as altereporene B.

Altereporene C (**3**), a yellowish-green powder, was designated with the molecular formula $C_{18}H_{26}O_4$, based on the HRESIMS analysis (*m*/*z* 329.1719 $[M + Na]^+$, calcd for 329.1723) with six degrees of unsaturation. The NMR data (Tables 1 and 2) indicated the presence of a highly similar skeleton like compound **2** except for the disappearance of the substituent at C-5 in **2** and the appearance of an additional hydroxy group at C-1 in **3**. This was substantiated by examination of upfield shift of C-1 (δ_C 63.8) in **3**, and the detailed inspection of ^1H–^1H COSY and HMBC correlations (Fig. 2). Then, the similar coupling constants and NOESY correlations with that of **2** (Fig. 3) suggested that the double bonds were 2*E* and 14*E* in **3** and it has two possible absolute configurations of 4*S*, 5*R*, 6*S*, 10*R*, 11*S*, 12*S*, 13*S*-**3** and 4*R*, 5*S*, 6*R*, 10*S*, 11*R*, 12*R*, 13*R*-**3**. Furthermore, with the identical specific rotations of the calculated and experimental results, the absolute configurations of **3** were assigned as 4*S*, 5*R*, 6*S*, 10*R*, 11*S*, 12*S*, 13*S*.

Altereporene D (**4**) was obtained as a white powder. The molecular formula of $C_{21}H_{28}O_4$ was assigned to **4** as determined by its HRESIMS (*m*/*z* 367.1885 $[M + Na]^+$, calcd for 367.1880), which corresponded to eight indices of hydrogen deficiency. Analysis of the ^{13}C NMR data revealed 21 carbon signals comprising four methyls, one methylene, eleven methines, three olefinic quaternary carbons, one oxygenated quaternary carbon and one aldehyde group. The NMR spectroscopic data (Tables 1 and 2) combined with the ^1H–^1H COSY and HMBC correlations (Fig. 2) suggested that **4** exhibited the very similar scaffold as compound **1**. The major difference was that a hydroxypropyl at C-4 (δ_C 137.6) in compound **1** instead by the aldehyde group at C-2 (δ_C 137.5) in **4**, which was supported by the HMBC correlations from H-1 to C-2 and H_3-19 to C-1/C-2/C-3. This assignment was further confirmed by the ^1H–^1H COSY and HMBC experiments (Fig. 2). *E*-geometry of double bonds at C_2–C_3, C_4–C_5, C_{16}–C_{17} and the relative configuration of **4** were designed as the same of **1** by the analysis of coupling constants and NOE correlations (Fig. 3). The determination of its absolute configuration also depended on the specific rotation test, the calculated specific rotation of 6*S*, 7*R*, 8*S*, 12*R*, 13*S*, 14*S*, 15*S*-**4**

was in good agreement with the experimental date, allowing confirmation of its absolute configuration, as shown in Fig. 1.

Altereporene E (**5**) was obtained as a white powder. Its molecular formula was deduced as $C_{21}H_{28}O_5$ based on its HRESIMS (*m/z* 383.1825 $[M + Na]^+$, calcd for 383.1829), indicating eight degrees of hydrogen deficiency. Detailed inspection of 1D and 2D NMR data of **5** with that of **4** revealed that they were structural analogues, with the obvious difference being that the absence of the aldehyde signal in **4** and the presence of a carboxyl at C-2 in **5**. It was verified by the HMBC correlations from H-3 and H-19 to C-1. A detailed 2D NMR analysis further constructed the structure of **5** (Fig. 2). Then, the absolute configuration of **5** was determined as the same of **4** to be 2*E*, 4*E*, 16*E*, 6*S*, 7*R*, 8*S*, 12*R*, 13*S*, 14*S*, and 15*S* by the analysis of NMR data and specific rotation calculation.

In the bioassays, the *in vitro* cytotoxic activities against five human tumor cell lines, anti-acetylcholinesterase activities and anti-inflammatory activities of compounds **1–5** were evaluated, but none showed significant inhibitory activities (details see ESI†).

Conclusions

In conclusion, a chemical investigation of endophytic fungus *Alternaria* sp. YUD20002 led to the isolation and identification of five new secondary metabolites altereporenes A–E (**1–5**). Their structures with absolute configurations were established. Further studies related to their bioactivities revealed all compounds **1–5** showed no significant inhibitory activities. However, the discovery of structurally interesting epoxy octahydronaphthalene derivatives extended the diversities in the family of the secondary metabolites from endophytic fungi with similar skeleton.

Experimental section

General experimental procedures

Specific rotations were measured with a Jasco model 1020 digital polarimeter (Horiba, Tokyo, Japan). One-dimensional and two-dimensional nuclear magnetic resonance (NMR) spectra were obtained on Bruker DRX-400 MHz (Bruker, Karlsruhe, Germany) spectrometers with tetramethylsilane (TMS) as an internal standard. UV-vis spectra were recorded using a Shimadzu UV-2550 PC spectrometer (Shimadzu Co., Ltd, Tokyo, Japan). HRESIMS data were obtained on an Agilent G3250AA (Agilent, Santa Clara, CA, USA). Electronic circular dichroism (ECD) spectra were measured with an Applied Photophysics Chirascan spectrometer (Applied Photophysics Ltd, UK). The preparative HPLC was performed on an Agilent 1260 series equipped with a DAD detector and a Zorbax SB-C18 (250 × 9.4 mm, 5 μm) semipreparative column. Sephadex LH-20 (GE Healthcare Co, Buckinghamshire, UK) and silica gel (200–300 mesh, Qingdao Marine Chemical Group Co., Qingdao, China) were applied for column chromatography. Fractions were monitored by TLC (GF254, Qingdao Haiyang Chemical Co. Ltd), with spots were detected by spraying with 10% H_2SO_4 in ethanol, followed by heating.

Fungal material

The fungal strain YUD20002 was isolated from the *Solanum tuberosum* which was collected from Kunming, Yunnan Province, China, in October 2020. The species of the strain was identified as *Alternaria* sp. based on the morphological method and reinforced by 18S rDNA along with internal transcribed spacer (ITS) sequences (GenBank No. ON204165). The strain YUD20002 was preserved at the School of Chemical Science and Technology, Yunnan University, China.

Fermentation, extraction and isolation

The fungus was inoculated in 3 × 500 mL Erlenmeyer flasks, each containing 100 mL of potato dextrose broth. Flask cultures were incubated at 28 °C on a rotary shaker at 160 rpm for 3 days as seed culture. Large-scale fermentation was carried out in 100 Erlenmeyer flasks (1000 mL), each contained rice (65 g), which were soaked overnight before autoclaving at 121 °C for 30 min. After cooling to room temperature, those Erlenmeyer flasks were respectively inoculated 3 mL seed broth, furthermore, which were maintained for 45 days at room temperature statically for chemical investigation.

The whole fermented culture was extracted with methanol, the extract was exhaustively extracted three times with EtOAc (1 day each time), after evaporating the organic solvent under vacuum, the crude extract (30 g) was obtained. The residue was subjected to silica gel column chromatography, eluted with a gradient of CH_2Cl_2–MeOH (1 : 0 to 0 : 1 *v/v*) to afford five fractions (Fr.1 to Fr.5).

Fr.1 was subjected to Sephadex LH-20 eluted with MeOH, silica gel CC (300–400 mesh) with a gradient elution of PE-EtOAc (20 : 1 to 0 : 1 *v/v*) and further purified by RP-HPLC with MeOH–H_2O (65 : 35 *v/v*) to obtain compound **4** (2.0 mg). Fr.3 was divided into four fractions (Fr.3-1 to Fr.3-4) by Sephadex LH-20 (in MeOH). Fr.3-3 was chromatographed on silica gel CC with a gradient elution of PE-EtOAc (10 : 1 to 0 : 1 *v/v*) and further isolated by RP-HPLC with MeOH–H_2O (65 : 35–85 : 15 *v/v*) to give compound **1** (4.2 mg). Fr.3-4 was separated on silica gel CC eluted with PE–EtOAc (10 : 1 to 0 : 1 *v/v*) and then purified by RP-HPLC with MeOH–H_2O (63 : 37 *v/v*) to provide compound **5** (3.9 mg). Compounds **2** (7.8 mg) and **3** (3.3 mg) were yield from Fr.4 through Sephadex LH-20 with MeOH elution and RP-HPLC (MeOH–H_2O, 45 : 55–75 : 25 *v/v*).

Altereporene A (**1**): white powder; [*a*] −121.0 (c 0.14, MeOH); UV (MeOH) λ_{max} (log ε) 242 (2.44) nm; HRESIMS *m/z* 397.2350 $[M + Na]^+$ (calcd for $C_{23}H_{34}O_4Na$, 397.2349); ^1H NMR (CD_3OD, 400 MHz) and ^{13}C NMR (CD_3OD, 100 MHz) in Tables 1 and 2.

Altereporene B (**2**): yellowish-green solid; [*a*] −105.3 (c 0.14, MeOH); UV (MeOH) λ_{max} (log ε) 195 (2.47) nm; HRESIMS *m/z* 410.2301 $[M + Na]^+$ (calcd for $C_{23}H_{34}O_4Na$, 410.2302); ^1H NMR (CD_3OD, 400 MHz) and ^{13}C NMR (CD_3OD, 100 MHz) in Tables 1 and 2.

Altereporene C (**3**): yellowish-green powder; [*a*] −118.3 (c 0.12, MeOH); UV (MeOH) λ_{max} (log ε) 195 (2.38) nm; HRESIMS *m/z* 329.1719 $[M + Na]^+$ (calcd for $C_{23}H_{34}O_4Na$, 329.1723); ^1H NMR (CD_3OD, 400 MHz) and ^{13}C NMR (CD_3OD, 100 MHz) in Tables 1 and 2.

Altereporene D (**4**): white powder; [*a*] −204.9 (c 0.11, MeOH); UV (MeOH) λ_{max} (log ε) 284 (2.55) nm; HRESIMS *m*/*z* 367.1885 $[M + Na]^+$ (calcd for $C_{23}H_{34}O_4Na$, 367.1880); ^1H NMR (CD_3OD, 400 MHz) and ^{13}C NMR (CD_3OD, 100 MHz) in Tables 1 and 2.

Altereporene E (**5**): white powder; [*a*] −132.5 (c 0.15, MeOH); UV (MeOH) λ_{max} (log ε) 265 (2.42) nm; HRESIMS *m*/*z* 383.1825 $[M + Na]^+$ (calcd for $C_{23}H_{34}O_4Na$, 383.1829); ^1H NMR (CD_3OD, 400 MHz) and ^{13}C NMR (CD_3OD, 100 MHz) in Tables 1 and 2.

Cytotoxicity assay

The *in vitro* cytotoxicity assay was performed according to the MTS method in 96-well microplates. The cell survival assay was carried out with the previously reported MTT method.[22–24] Five human tumor cell lines, including human promyelocytic leukemia HL-60, human hepatocellular carcinoma SMMC-7721, lung cancer A-549, breast cancer MDA-MB-231, and human colon cancer SW480, were used in the cytotoxicity assays, and cisplatin was used as a positive control. All cells were cultured in RPMI-1640 or DMEM medium (Hyclone, Logan, UT, USA), supplemented with 10% fetal bovine serum (Hyclone) at 37 °C in a humidified atmosphere containing 5% CO_2. The cells were seeded onto 96-well plates at 1.5×10^4 cells per well and after 24 h the compounds were added in different concentrations of 0.064, 0.32, 1.6, 8, and 40 μM for 48 h at 37 °C. Subsequently, MTS was added to the culture medium and the absorbance at 490 nm was measured with a microplate reader. The proliferation rate was calculated as the ratio of absorbance to that of the control.

Acetylcholinesterase inhibitory activity

Acetylcholinesterase (AChE) inhibitory activities of the compounds **1–5** were assayed by using modified Ellman's method as described in a previous literature report.[25] *S*-Acetylthiocholine iodide, *S*-butyrylthiocholine iodide, 5,5′-dithiobis-(2-nitrobenzoic) acid (DTNB, Ellman's reagent), acetylcholinesterase derived from human erythrocytes were purchased from Sigma Chemical. Compounds were dissolved in DMSO. The reaction mixture (totally 200 μL) containing phosphate buffer (pH 8.0), test compound (50 μM), and acetyl cholinesterase (0.02 U mL^{-1}), was incubated for 20 min (37 °C). Then, the reaction was initiated by the addition of 40 μL of solution containing DTNB (0.625 mM) and acetylthiocholine iodide (0.625 mM) for AChE inhibitory activity assay, respectively. The hydrolysis of acetylthiocholine was monitored at 405 nm every 30 seconds for one hour. Tacrine was used as positive control with final concentration of 0.333 μM.

Anti-inflammatory assay

The *in vitro* anti-inflammatory activity of compounds **1–5** were performed by evaluating the inhibition of nitric oxide (NO) level in lipopolysaccharide (LPS)-induced RAW264.7 cells.[26] The cells were cultured in RPMI 1640 medium in 96-well plates at a density of 1×10^5 cells per well for 24 h, and LPS (Sigma-Aldrich, St. Louis, MO, USA) was added to the medium at a concentration of 1 μg mL^{-1} to induce inflammation, with L-NMMA used as the positive control. After 24 h, the cell culture supernatant was mixed with Griess reagent. The absorbance was measured at 570 nm by a microplate reader. The nitrite concentrations were calculated according to the method reported by Jin *et al.*[27] After we removed the cell culture supernatant out for NO examination, the cell viability by comparing to living cells in untreated groups was calculated to determine the cytotoxicity of tested compounds by MTS assays.

ECD calculations

The initial conformational distributions search were performed using CONFLEX software with the Merck molecular force-field (MMFF) 94 s force-field 5 kcal mol^{-1} above the ground state. The conformers were confirmed as energetic local minima through analytical inspection of their vibrational frequencies, the absence of imaginary frequencies confirms stationary state was found. These conformers were further optimized by the density functional theory (DFT) using Gaussian 09 at the B3LYP/6-31g (d, p) level.[28,29] The solvent effects of the methanol solution were taken into account using the polarizable continuum model (PCM). The stable conformers (5 kcal mol^{-1} energy threshold) obtained were submitted to ECD calculation at the B3LYP/6-31g (d, p) level. The calculated ECD spectra were produced by SpecDis 1.64 software and compared to the experimental data.[25]

Optical rotation calculations

Each isomer was optimized using DFT at the B3LYP/6-31g (d, p) level in the Gaussian 09 program. Methanol was used as a solvent with the polarizable continuum solvent model (PCM). Then, the optimized isomer was calculated using TDDFT/GIAOs at the B3LYP/6-31g* in the Gaussian 09 program to generate its specific rotation.[30]

Conflicts of interest

There are no conflicts to declare.

Acknowledgements

This work was financially supported by grants from the Natural Science Foundation of China (No. 81860623), the Program for Innovative Research Team of Yunnan Province (202105AE160006), the project of Yunling Scholars of Yunnan province, a grant from the Science and Technology Project of Yunnan Provincial Department of Science and Technology (No. 202101AT070629), the Open Project of Yunnan Clinical Medical Center (2020LCZXKF-HX02) and the Science and Technology project of Yunnan Province (202101AY070001-246). Authors thank Advanced Analysis and Measurement Center of Yunnan University for the sample testing service.

References

1 A. H. Aly, A. Debbab and P. Proksch, *Pharmazie*, 2013, **68**, 499–505.

2 S. Kusari, C. Hertweck and M. Spiteller, *Chem. Biol.*, 2012, **19**, 792–798.
3 G. Li, S. Kusari, M. Lamshöft, A. Schüffler, H. Laatsch and M. Spiteller, *J. Nat. Prod.*, 2014, **77**, 2335–2341.
4 C. Klemke, S. Kehraus, A. D. Wright and G. M. König, *J. Nat. Prod.*, 2004, **67**, 1058–1063.
5 G. Strobel, B. Daisy, U. Castillo and J. Harper, *J. Nat. Prod.*, 2004, **67**, 257–268.
6 J. Fischer, V. Schroeckh and A. A. Brakhage, *Gene Expression Systems in Fungi: Advancements and Application*, Springer International Publishing, Springer, 2016, pp. 253–273.
7 S. Chen, H. Li, Y. Chen, S. Li, J. Xu, H. Guo, Z. Liu, S. Zhu, H. Liu and W. Zhang, *Bioorg. Chem.*, 2019, **86**, 368–374.
8 A. H. Aly, R. Edrada-Ebel, I. D. Indriani, V. Wray, W. E. G. Müller, F. Totzke, U. Zirrgiebel, C. Schächtele, M. H. G. Kubbutat, W. H. Lin, P. Proksch and R. Ebel, *J. Nat. Prod.*, 2008, **71**, 972–980.
9 X. Lu, X.-Y. Tang, H.-X. Wang, W.-J. Huang, W.-X. Feng and B.-M. Feng, *Bioorg. Chem.*, 2021, **116**, 105309.
10 F. Li, Y. Tang, W. Sun, J. Guan, Y. Lu, S. Zhang, S. Lin, J. Wang, Z. Hu and Y. Zhang, *Bioorg. Chem.*, 2019, **92**, 103279.
11 M. M. Gamboa-Angulo, F. A. lejos-González, F. Escalante-Erosa, K. García-Sosa and L. M. Pea-Rodríguez, Novel dimeric metabolites from *Alternaria tagetica*, *J. Nat. Prod.*, 2000, **63**, 1117–1120.
12 C. J. Zheng, C. L. Shao, Z. Y. Guo, J. F. Chen, D. S. Deng, K. L. Yang, Y. Y. Chen, X. M. Fu, Z. G. She, Y. C. Lin and C. Y. Wang, *J. Nat. Prod.*, 2012, **75**, 189–197.
13 L. M. Abreu, R. K. Phipp and L. H. Pfernning, *Tetrahedron Lett.*, 2010, **51**, 1803–1805.
14 Z. Hu, W. Sun, F. Li, J. Guan, Y. Lu, J. Liu, Y. Tang, G. Du, Y. Xue, Z. Luo, J. Wang, H. Zhu and Y. Zhang, *Org. Lett.*, 2018, **20**, 5198–5202.
15 F. Li, W. Sun, J. Guan, Y. Lu, S. Zhang, S. Lin, J. Liu, W. Gao, J. Wang, Z. Hu and Y. Zhang, *Org. Lett.*, 2018, **20**, 7982–7986.
16 F. Li, Z. Ye, Z. Huang, X. Chen, W. Sun, W. Gao, S. Zhang, F. Cao, J. Wang, Z. Hu and Y. Zhang, *Bioorg. Chem.*, 2021, **117**, 105452.
17 Y. Shiono, *Chem. Biodiversity*, 2006, **3**, 217–223.
18 J. Xu, F. Ji, J. Kang, H. Wang, S. Li, D. Q. Jin, Q. Zhang, H. Sun and Y. Guo, *J. Agric. Food Chem.*, 2015, **63**, 5805–5812.
19 X. Y. Wang, T. T. Xu, L. J. Sun, R. H. Cen, S. Su, X. Q. Yang, Y. B. Yang and Z. T. Ding, *Bioorg. Chem.*, 2021, **114**, 105148.
20 H. T. Li, L. H. Tang, T. Liu, R. N. Yang, Y. B. Yang, H. Zhou and Z. T. Ding, *Bioorg. Chem.*, 2020, **95**, 103503.
21 J. S. Puranen, M. J. Vainio and M. S. Johnson, *J. Comput. Chem.*, 2010, **31**, 1722–1732.
22 B. Yang, W. Sun, J. Wang, S. Lin, X. N. Li, H. Zhu, Z. Luo, Y. Xue, Z. Hu and Y. Zhang, *Mar. Drugs*, 2018, **16**, 110.
23 A. H. Cory, T. C. Owen, J. A. Barltrop and J. G. Cory, *Cancer Commun.*, 1991, **3**, 207–212.
24 Y. Ren, J. C. Gallucci, X. Li, L. Chen, J. Yu and A. D. Kinghorn, *J. Nat. Prod.*, 2018, **81**, 554–561.
25 H. T. Li, L. Tang, T. Liu, R. Yang, Y. Yang, H. Zhou and Z. T. Ding, *Org. Chem. Front.*, 2019, **6**, 3847–3853.
26 Y. Chen, Z. M. Liu, H. J. Liu, Y. H. Pan, J. Li, L. Liu and Z. G. She, *Mar. Drugs*, 2018, **16**, 54.
27 X. Jin, S. Q. Song, J. Wang, Q. Z. Zhang, F. Qiu and F. Zhao, *Exp. Ther. Med.*, 2016, **12**, 499–505.
28 M. E. Ochoa, P. Labra-Vázquez, N. Farfan and R. Santillan, *Cryst. Growth Des.*, 2018, **5**, 2795–2803.
29 P. Labra-Vázquez, A. Z. Lugo-Aranda, M. Maldonado-Domínguez, R. Arcos-Ramos, M. D. P. Carreon-Castro, R. Santillan and N. Farfán, *J. Mol. Struct.*, 2015, **1101**, 116–123.
30 H. Zhou, Y. B. Yang, R. T. Duan, X. Q. Yang, J. C. Zhang, X. G. Xie and Z. T. Ding, *Chin. Chem. Lett.*, 2016, **27**, 1044–1047.